

Learning from Neighbors: Category Extrapolation for Long-Tail Learning

Shizhen Zhao¹ Xin Wen¹ Jiahui Liu¹ Chuofan Ma¹ Chunfeng Yuan² Xiaojuan Qi^{1*}

¹ The University of Hong Kong

² National Laboratory of Pattern Recognition, Institute of Automation, Chinese Academy of Sciences
{zhaosz, xjq}@eee.hku.hk

Abstract

Balancing training on long-tail data distributions remains a long-standing challenge in deep learning. While methods such as re-weighting and re-sampling help alleviate the imbalance issue, limited sample diversity continues to hinder models from learning robust and generalizable feature representations, particularly for tail classes. In contrast to existing methods, we offer a novel perspective on long-tail learning, inspired by an observation: datasets with finer granularity tend to be less affected by data imbalance. In this paper, we investigate this phenomenon through both quantitative and qualitative studies, showing that increased granularity enhances the generalization of learned features in tail categories. Motivated by these findings, we propose a method to increase dataset granularity through category extrapolation. Specifically, we introduce open-set fine-grained classes that are related to existing ones, aiming to enhance representation learning for both head and tail classes. To automate the curation of auxiliary data, we leverage large language models (LLMs) as knowledge bases to search for auxiliary categories and retrieve relevant images through web crawling. To prevent the overwhelming presence of auxiliary classes from disrupting training, we introduce a neighbor-silencing loss that encourages the model to focus on class discrimination within the target dataset. During inference, the classifier weights for auxiliary categories are masked out, leaving only the target class weights for use. Extensive experiments on three standard long-tail benchmarks demonstrate the effectiveness of our approach, notably outperforming strong baseline methods that use the same amount of data. The code will be made publicly available.

1. Introduction

Deep models have shown extraordinary performance on large-scale curated datasets [10, 11, 18, 33]. But when

*Corresponding author

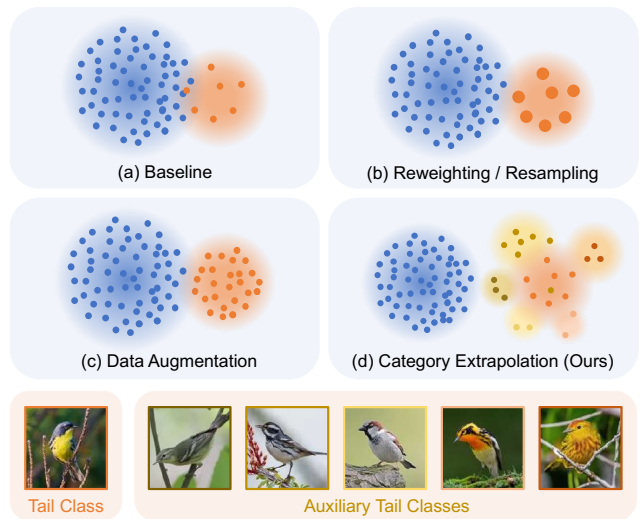


Figure 1. Holistic comparison to previous philosophy. (a) Data imbalance between head and tail classes makes biased features; (b), (c): Previous methods are still bounded by existing known classes; (d) We instead seek help from auxiliary open-set data.

dealing with real-world applications, they generally face highly imbalanced (e.g., long-tailed) data distribution: instances are dominated by a few head classes, and most classes only possess a few images [9, 12, 38, 39]. Learning in such an imbalanced setting is challenging as the instance-rich (or head) classes dominate the training procedure [1, 6, 31, 44]. Without considering this situation, models tend to classify tailed class samples as similar head categories, leading to significant performance degradation on tail categories [26, 27, 41, 47].

Existing works tackle challenges in long-tail learning from various perspectives. An earlier stream is to re-balance the learning signal (e.g., re-weighting [7] and re-sampling [3]). Yet, they inevitably face the scarcity of data and suffer from over-fitting on tail classes (Fig. 1b). Another straightforward fix is to augment training samples into diverse ones through image transformations [4, 8, 42, 43]. These methods typically increase the loss weights or en-

hance the sample diversity of tail classes to balance representation learning (Fig. 1c). Despite advances, limited sample diversity still constrains the ability to generalize the learned features. Additionally, improvements in tail class performance are often accompanied by a decline in head class performance. This limitation motivates us to investigate what factors contribute to generalizable feature learning in long-tail settings. Our insight is inspired by a common, yet counterintuitive, phenomenon observed in existing benchmarks: despite being more imbalanced than ImageNet-LT [20], iNat18 [36] achieves nearly balanced performance (see Tab. 1). This observation raises the question: *Does granularity play a role in the performance balance of long-tail learning?*

Dataset	#Class	#Train	Granul.	Imb. Factor β	Many	Med.	Few
IN-LT	1000	116K	Coarse	1280/5=256	68.2	56.8	41.6
iNat18	8142	438K	Fine	1000/2=500	70.3	71.3	70.2

Table 1. Average performance of previous methods.

To investigate this further, we conducted a pilot study (see Sec. 2.2) using a larger data pool and controlled experiments to verify this phenomenon. We found that datasets with finer granularity are less affected by data imbalance. Feature visualizations (see Fig. 2) reveal that, despite a long-tail distribution, datasets with finer granularity enable the model to learn more generalized representations. This discovery motivates us to explore *altering data distribution by introducing open-set categories to increase the granularity of data for long-tail learning.*

At the core of our approach is the idea of augmenting training data with fine-grained categories related to the original ones, thereby increasing granularity (Fig. 1d). To acquire auxiliary data, we establish a fully automated data crawling pipeline powered by the knowledge of large language models (LLMs). Specifically, for each class to be expanded, we query an LLM for k fine-grained auxiliary classes, then retrieve corresponding images from the web based on these class names (Fig. 4). The crawled data are subsequently integrated with the original dataset for model training. During training, we introduce a neighbor-silencing loss to enhance discrimination between confusing classes, prevent the model from being overwhelmed by auxiliary classes, and ensure alignment with the objectives of the testing phase. After training, the classifier by simply masking out the auxiliary classes demonstrates strong performance without the need for additional classifier re-balancing, as required in previous methods [14, 46].

Intuitively, our method could be interpreted as *category extrapolation*. These augmented categories complete the learning signal, which may fill the gap between originally distinct classes, encourage continuity and smoothness of the feature manifold, and allow better generalization of repre-

sentations across classes. In terms of classification, samples of auxiliary classes take up the neighborhood of existing classes, thus explicitly enlarging the margin between them and encouraging discriminability. Empirically, we indeed observe tighter clusters and better separation in-between (Fig. 2d).

Our major contributions are summarized as follows:

- We explore the effect of granularity on the performance balance in long-tail learning, which motivate us to introduce neighbor classes to increase the granularity and facilitate representation learning for both head and tail classes.
- We propose a neighbor-silencing learning loss to facilitate long-tail learning with extra open-set categories and design a fully automatic data acquisition pipeline to efficiently harvest data from the Web.
- We conduct extensive experiments across standard benchmarks using various training paradigms (*e.g.*, random initialization, CLIP [28], and DINOv2 [23]), all of which consistently demonstrate high performance.

2. Pilot Study

In this section, we investigate whether granularity impacts performance balance in long-tail distribution. We first provide preliminary for long-tail learning and an analysis on a baseline method in Sec. 2.1. Then, we verify the impact of the granularity of training data on long-tail learning (Sec. 2.2) from both quantitative and qualitative perspectives.

2.1. Preliminary

In long-tail visual recognition, the model has access to a set of N training samples $\mathcal{S} = \{(\mathbf{x}_n, y_n)\}_{n=1}^N$, where $\mathbf{x}_n \in \mathcal{X} \subset \mathbb{R}^D$ and labels $\mathcal{Y} = \{1, 2, \dots, L\}$. Training class frequencies are defined as $N_y = \sum_{(\mathbf{x}_n, y_n) \in \mathcal{S}} \mathbb{1}_{y_n=y}$ and the test-class distribution is assumed to be sampled from a uniform distribution over \mathcal{Y} , but is not explicitly provided during training. A classic solution is to minimize the balanced error (BE), of a scorer $\mathbf{f} : \mathcal{X} \rightarrow \mathbb{R}^L$, defined as:

$$\text{BE}(\mathbf{x}, \mathbf{f}(\cdot)) = \sum_{y \in \mathcal{Y}} \mathbf{P}_{\mathbf{x}|y} \left(y \notin \arg \max_{y' \in \mathcal{Y}} \mathbf{f}_{y'}(\mathbf{x}) \right), \quad (1)$$

where $\mathbf{f}_y(x)$ is the logit produced for true label y for sample \mathbf{x} . Traditionally, this is done by minimizing a proxy loss, the Balanced Softmax Cross Entropy (BalCE) [7]:

$$\begin{aligned} \mathcal{L}_{\text{BalCE}}(\mathcal{M}(\mathbf{x}|\theta_f, \theta_w), \mathbf{y}_i) &= -\log[p(\mathbf{y}_i|\mathbf{x}; \theta_f, \theta_w)] \\ &= -\log \left[\frac{n_{\mathbf{y}_i} e^{z_{\mathbf{y}_i}}}{\sum_{\mathbf{y}_j \in \mathcal{Y}} n_{\mathbf{y}_j} e^{z_{\mathbf{y}_j}}} \right] \\ &= \log \left[1 + \sum_{\mathbf{y}_j \neq \mathbf{y}_i} e^{\log n_{\mathbf{y}_j} - \log n_{\mathbf{y}_i} + z_{\mathbf{y}_j} - z_{\mathbf{y}_i}} \right]. \end{aligned} \quad (2)$$

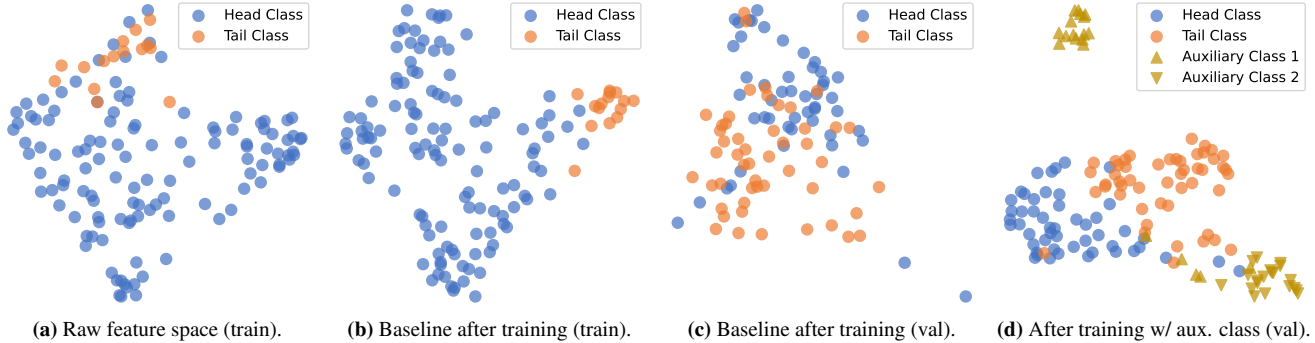


Figure 2. Feature visualization of confusing head and tail classes by UMAP [24] on ImageNet-LT [20]. (a) Raw feature space of training data by DINOv2 [23]; (b) Feature space of training data after the training phase; (c) The baseline (re-weighting) shows poor generalization on validation data; (d) Adding auxiliary categories condenses clusters and improves separation.

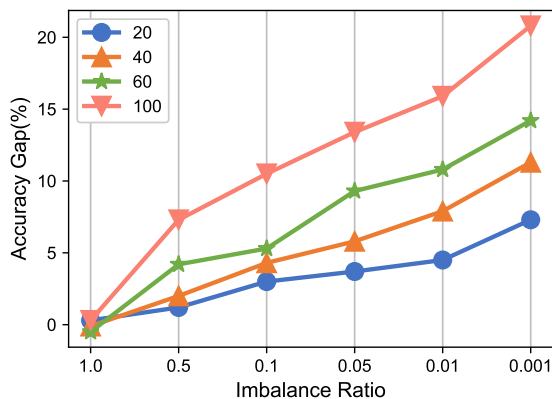


Figure 3. Effect of granularity vs. imbalance ratio.

This is known as *re-weighting*, where the contribution of each label’s individual loss is scaled by an inverse class frequency derived from the class’s instance number n_{y_i} . We adopt this setting as the baseline in follow-up experiments.

On the failure of re-balancing. The primary challenge of long-tail learning stems from data imbalance, which affects the representation learning of both head classes and few-shot classes. For head classes, if there is a lack of effective negative-class samples, then learning an effective boundary is challenging. To better demonstrate this, we provide feature visualizations of confusing head (*Scottish Deerhound*) and tail (*Irish Wolfhound*) classes on ImageNet-LT in Fig. 2. As in Fig. 2a, these two classes are challenging even for the advanced vision foundation model DINOv2 [23]. After training with the re-weighting baseline on the imbalanced training data, the learned features seem relatively satisfactory (Fig. 2b). However, the generalization is poor: samples in the validation data are still convoluted, and the separation between them is unclear (Fig. 2c). On top of this baseline, we then study the effect of data distribution on long-tail learning.

2.2. Granularity Matters in Long-Tail learning

We study whether the granularity of the dataset is critical to long-tail learning. Our study is motivated by an intriguing observation that, although more classes and stronger imbalance, we observe nearly balanced performance on iNat18 [36], as opposed to ImageNet-LT [20]. A significant distinction is that iNat18 is an extremely fine-grained dataset with over 8000 categories, yet it only consists of 14 superclasses in total. On the other hand, ImageNet-LT, although comprising only 1000 categories, has over 100 superclasses, making it relatively coarse-grained. Therefore, we conduct experiments to study the effect of granularity on long-tail learning.

Dataset Configuration. To this end, we construct a dataset pool using ImageNet-21k [29] and OpenImage [15] datasets. To investigate the influence of granularity, we sample 500 classes from the pool for each time and control the number of superclasses to be $\{20, 40, 60, 100\}$ based on WordNet. Then, we used different imbalance ratios $\{1.0, 0.5, 0.1, 0.05, 0.01, 0.001\}$ to study the effect of granularity on the imbalance ratio. We train the model (ViT-Base [10]) using BalCE [7] as Eq. (2). We conduct 5 experiments and take the average value.

In Fig. 3, we show the performance gap between head categories and tail categories under different dataset imbalance ratios. The results show that as the granularity increases, the dataset is less sensitive to the imbalance ratio. For example, when the number of superclasses is 20, the performance gap between the head and tail is 7.3%, while the gap is 20.8% when the number of superclasses is 100, under the severe imbalance (imbalance ratio=0.001).

Finding 1: Increased granularity of training data benefits long-tail learning.

In a fine-grained long-tail dataset, although there are few samples for tail categories, many categories share similar patterns, which is conducive to learning distinctive features,

thus enhancing generalizability. As reflected in Fig. 2d, for clearer visualization, we sample two fine-grained categories that is denoted as the auxiliary classes. The visualization shows that the separation between head and tail classes is clearly improved. Also, the distribution of intra-class samples is also more compact. Due to the space limitation, we show more examples in Appendix. This motivate us to introduce diverse open-set auxiliary categories to enhance the granularity for close-set long-tail learning.

Finding 2: Despite long-tail distribution, increased granularity could explicitly separate and condensify existing data clusters.

Based on the above findings, given a long-tail dataset, we aim to establish a framework that can effectively acquire auxiliary data to enhance the granularity. Specifically, we utilize LLMs to query the candidate auxiliary categories and crawl images from the Web, followed by a filtering stage to ensure similarity and diversity. To better incorporate auxiliary data for training with target categories, we propose a Neighbor-Silencing Loss to avoid being overwhelmed by auxiliary classes. Details are included in Sec. 3.

3. Long-Tail Learning by Category Extrapolation

In this section, we first introduce our simple and automatic pipeline for obtaining auxiliary data in Sec. 3.1. Then, we present our new learning objective that effectively leverages the auxiliary data to enhance long-tail learning in Sec. 3.2.

3.1. Neighbor Category Searching

In search of neighbor categories sharing some common visual patterns with the pre-defined categories in the dataset, we design a fully automatic crawling pipeline that includes (i) querying neighbor categories from LLMs to obtain similar categories and enhance the granularity of the training data and (ii) retrieving corresponding images from the web and conducting filtering to guarantee similarity and diversity. An overview of this pipeline is illustrated in Fig. 4, and we introduce each step in detail as follows.

Querying LLM for Neighbor Categories. We take advantage of the recent development of Large Language Models (LLMs), *e.g.*, GPT-4 [25], and query them for expert knowledge of possible fine-grained classes with respect to the classes to extrapolate (*i.e.*, the medium and tail classes by default). For example, we can prompt the language model with: “Please create a list which contains 5 fine-grained categories related to {CLS}”. However, the output of this naive prompt is unstable, possibly because ‘fine-grained categories’ by itself is quite a broad and vague concept. To make the prompt more concrete and clear for LLMs, we design a structural prompt with in-context learning:

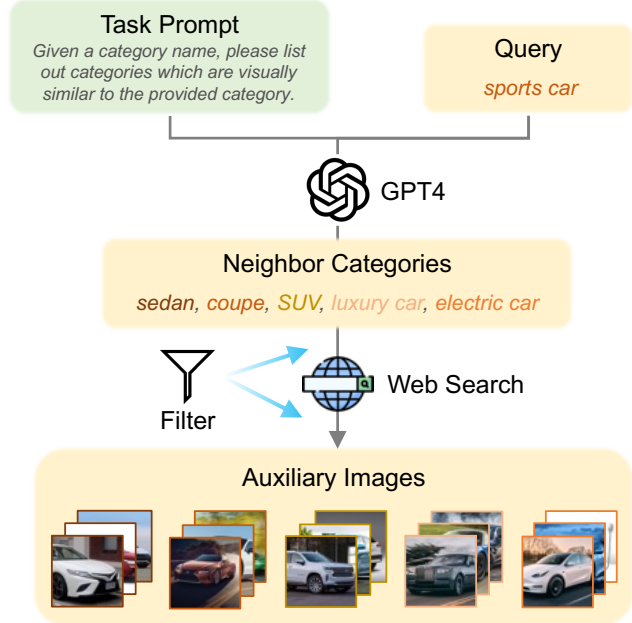


Figure 4. Data crawling pipeline. We prompt GPT-4 [25] for fine-grained categories related to query classes and retrieve corresponding images from the web. Classes already in the label set and images of lower visual similarity than the threshold are filtered out.

Task: Given a category name, please list out 5 classes that are fine-grained categories related to the provided classes.

Query: sports car

Response: sedan, coupe, SUV, luxury car, electric car

Query: {CLS}

Response:

The LLM then completes the response above. After that, classes in the target dataset \mathcal{S} are filtered out to avoid possible information leaks. Then, the remaining class names are fed to an image-searching engine for image retrieval.

Retrieving and Filtering Images from the Web. Images retrieved by the search engine can be noisy, thus, a filtering strategy is adopted. An image \mathbf{x}_r corresponding to a specific class y_i is dropped if: (i) the class’s name does not exist in the associated caption; or (ii) the visual similarity between the class and this image satisfies thresholds: $\gamma_1 < \cos(\mathbf{p}_i, \mathbf{f}_r) < \gamma_2$. We employ DINOv2 [23] for feature extraction and use cosine similarity as the metric. Specifically, the prototype \mathbf{p}_i of category y_i is computed as the average feature of all samples of this category in the target dataset \mathcal{S} : $\mathbf{p}_i = 1/n_{y_i} \sum_j \mathbf{f}_j$. After the filtering process, the model has access to a set of M auxiliary training samples $\mathcal{A} = \{(\mathbf{x}_m, y_m)\}_{m=1}^M$, where $\mathbf{x}_m \in \mathcal{X} \subset \mathbb{R}^D$ and

labels $\mathcal{Y}_a = \{L + 1, L + 2, \dots, L + K\}$ and the category number for auxiliary set is K .

3.2. Learning with Auxiliary Categories

We mix the auxiliary dataset \mathcal{A} and the target dataset \mathcal{S} for training. A naive approach is to directly employ the BalCE loss [7] by merging the label space:

$$\mathcal{L}_{\text{BalCE}} = -\log \left[n_{\mathbf{y}_i} e^{z_{\mathbf{y}_i}} / \left(\overbrace{\sum_{\mathbf{y}_j \in \mathcal{Y}} n_{\mathbf{y}_j} e^{z_{\mathbf{y}_j}}}^{\text{Target}} + \overbrace{\sum_{\mathbf{y}_j \in \mathcal{Y}_a} n_{\mathbf{y}_j} e^{z_{\mathbf{y}_j}}}^{\text{Auxiliary}} \right) \right]. \quad (3)$$

But note that our objective is to classify L categories within the target dataset, as opposed to $L + K$ categories. Directly employing the standard BalCE loss as Eq. (3) would result in an inconsistency between the optimization process and the ultimate goal. The auxiliary part could overwhelm optimization and result in degenerated performance. We thus “silent” them by weighting as follows.

Silencing the Overwhelming Neighbors. Concretely, if y_j is a neighbor category of y_i from auxiliary categories, we spot this as possible neighbor overwhelming and give the corresponding logit a smaller weight. To clarify, y_j is a neighbor category of y_i means that y_j is queried from y_i by Neighbor Category Searching (Sec. 3.1). We thus expect the auxiliary classes to influence less the target class which they are queried from, and contribute more to their classification as a whole with respect to other classes. The neighbor-silencing variant of the re-balancing loss is then formulated as:

$$\mathcal{L}_{\text{NS-CE}} = \log \left[1 + \sum_{\mathbf{y}_j \neq \mathbf{y}_i} \lambda_{ij} \cdot e^{\log n_{\mathbf{y}_j} - \log n_{\mathbf{y}_i} + z_{\mathbf{y}_j} - z_{\mathbf{y}_i}} \right], \quad (4)$$

where $\lambda_{ij} = \lambda_s$, if y_i and y_j satisfy that one is the other’s neighbor category and one of them from auxiliary categories, and $\lambda_{ij} = 1$ otherwise. λ_s is the weight for balancing the loss between neighbor category pairs and non-pairs. By default, $0 < \lambda_s < 1$. In this way, we assign a smaller weight to neighbor category pairs, thus, the effect within neighbor classes is weakened, and the optimization focuses more on their separation as a whole from other confusing classes.

Obtaining the Final Classifier. Given that our model’s classifier includes more categories, it cannot be directly applied to the target dataset for evaluation. A common practice is to discard the trained classifier and re-train it with re-balancing techniques on the target dataset through linear probing [14, 46]. However, this could be suboptimal since the separation hyper-planes shaped by auxiliary categories can be undermined. Therefore, we try directly masking out the weights of auxiliary categories, retaining only

the weights of the target categories. Specifically, we denote the trained classifier weights as $\mathcal{W} = \{\mathbf{w}_i\}_{i=1}^{L+K}$, where $\mathbf{w}_i \in \mathbb{R}^C$, and keep $\mathcal{W} = \{\mathbf{w}_i\}_{i=1}^L$. Surprisingly, this simpler approach works better. This is potentially because incorporating more auxiliary fine-grained categories can enable the classifier to focus on class-specific discriminative features. These features possess stronger generalizability, facilitating the classifier to construct more precise separation hyper-planes.

4. Experiments

4.1. Datasets

We experiment with three standard long-tailed image classification benchmarks. We report accuracy on three splits of the set of classes: Many-shot (more than 100 images), Medium-shot (20~100 images), and Few-shot (less than 20 images). Besides, we also report the commonly used top-1 accuracy over all classes for evaluation.

ImageNet-LT [20] is a class-imbalanced subset of the popular image classification benchmark ImageNet ILSVRC 2012 [30]. The images are sampled following the *Pareto* distribution with a power value $\alpha = 6$, containing 115.8k images from 1,000 categories. **iNaturalist 2018** [36] (iNat18 for short) is a species classification dataset, which consists of 437.5k images from 8,142 fine-grained categories following an extreme long-tail distribution. **Places-LT** is a synthetic long-tail variant of the large-scale scene classification dataset Places [45]. With 62.5k images from 365 categories, its class cardinality ranges from 5 to 4,980.

4.2. Implementation Details

We adopt ViT-Base [10] as the backbone. Our models are trained with the AdamW optimizer [22] with $\beta_s = \{0.9, 0.95\}$, with an effective batch size of 512. We train all models with RandAug(9, 0.5) [5], Mixup(0.8) [43] and Cutmix(1.0) [42]. We set the maximum sampling number for each auxiliary category to 50 in each training epoch. For the ratio of neighbor category for head, medium, and tail class, we set to $1 : \left\lceil \frac{N_h}{N_m} \right\rceil : \left\lceil \frac{N_h}{N_t} \right\rceil$, where N_h , N_m , and N_t denote the total number of samples of head, medium, and tail classes, respectively. $\lceil \cdot \rceil$ stands for ceiling, which rounds a number up to the nearest integer. Following LiVT [40], the training epochs for ImageNet-LT, iNaturalist, and Places-LT is set to 100, 100, and 30, respectively. The hyper-parameter λ_s is set to 0.1. γ_1 and γ_2 are set to 0.7 and 0.98. See detailed implementation settings in the Appendix.

4.3. Main Results

Comparison with Baseline with Different Pre-training. We experiment with three different pre-training paradigms (*i.e.*, random initialization, CLIP [28], and DINOv2 [23]). The baseline applies Bal-CE [7] loss. As shown in Tab. 2,

Method	ImageNet-LT				iNaturalist 18				Place-LT				
	Overall	Many	Med.	Few	Overall	Many	Med.	Few	Overall	Many	Med.	Few	
Scratch	Baseline	60.9	72.9	56.8	41.4	76.1	78.5	76.9	74.6	39.9	43.0	40.5	33.3
	+ RD	56.8	72.1	50.4	35.8	68.4	76.4	70.1	64.3	36.5	41.9	36.1	27.5
	+ SD	64.9	73.4	62.1	50.6	76.8	78.6	77.2	75.7	41.6	43.4	42.1	36.9
	+ Ours	68.2 \uparrow 7.3	74.5 \uparrow 1.6	66.2 \uparrow 9.4	57.4 \uparrow 16.0	78.0 \uparrow 1.9	78.9 \uparrow 0.4	78.2 \uparrow 1.3	77.5 \uparrow 2.9	43.8 \uparrow 3.9	43.7 \uparrow 0.7	44.8 \uparrow 4.3	41.6 \uparrow 8.3
CLIP	Baseline	74.0	77.2	72.8	68.5	75.0	77.8	76.5	72.5	48.4	47.9	48.6	48.9
	+ RD	68.8	75.4	67.4	55.2	67.7	75.1	69.8	63.1	43.3	45.1	43.4	40.2
	+ SD	75.2	77.8	74.2	71.3	76.7	78.5	77.9	74.6	49.2	48.7	49.5	49.4
	+ Ours	77.3 \uparrow 3.5	79.1 \uparrow 1.9	76.8 \uparrow 4.0	74.1 \uparrow 5.6	78.5 \uparrow 3.5	79.5 \uparrow 1.5	79.3 \uparrow 2.8	77.3 \uparrow 4.8	50.5 \uparrow 2.1	50.0 \uparrow 2.1	51.0 \uparrow 2.4	50.2 \uparrow 1.3
DINOv2	Baseline	79.6	84.3	78.3	71.1	85.0	85.7	86.2	84.2	49.5	49.2	51.3	46.1
	+ RD	77.2	83.3	75.7	65.4	75.4	82.3	76.1	72.6	45.2	47.2	45.2	41.3
	+ SD	80.5	83.8	79.8	73.4	85.9	85.8	86.5	85.0	49.9	49.3	51.6	47.3
	+ Ours	82.0 \uparrow 2.4	84.7 \uparrow 0.4	81.5 \uparrow 3.2	76.2 \uparrow 5.1	87.0 \uparrow 2.0	86.4 \uparrow 0.7	87.4 \uparrow 1.2	86.7 \uparrow 2.5	50.8 \uparrow 1.3	49.4 \uparrow 0.2	52.4 \uparrow 1.1	49.2 \uparrow 3.1

Table 2. Quantitative results of the proposed method on three standard benchmarks. For each dataset, we conduct three pre-training paradigms (training from scratch, CLIP, and DINOv2) to compare our method with baseline methods on accuracy (%). In addition, we report the **relative improvement** of our method compared to the baseline method in each setting. RD denotes the random auxiliary data and SD is the data from our selected neighbor categories.

Methods	Backbone	Overall	Many	Med.	Few
Training from scratch					
LiVT [40]	ViT-B	60.9	73.6	56.4	41.0
LiVT \dagger [40]	ViT-B	65.2	73.7	62.8	49.8
Ours	ViT-B	68.2	74.5	66.2	57.4
Fine-tuning pre-trained model (CLIP)					
LIFT [32]	ViT-B	77.0	80.2	76.1	71.5
LIFT \dagger [32]	ViT-B	77.8	80.2	77.2	73.1
Ours	ViT-B	78.8	80.3	78.4	75.8
Fine-tuning pre-trained model (DINOv2)					
Bal-CE [7]	ViT-B	79.6	84.3	78.3	71.1
Bal-CE \dagger [7]	ViT-B	80.5	83.8	79.8	73.4
Ours	ViT-B	82.0	84.7	81.5	76.2

Table 3. Performance on ImageNet-LT. We report accuracy (%) of all methods under three pre-training paradigms. We also report the performance of adding the auxiliary data but without our method, which denotes by \dagger .

our method significantly improves the performance over the baseline on all three datasets, especially on fewer-shot classes. This improvement is also consistent and generalizes to a variety of pre-training strategies. In particular, when the model is trained from scratch, we observe a significant performance boost on ImageNet-LT, with a 16.0% increase in accuracy on the tail classes. A plausible explanation is that randomly initialized networks are more prone to overfitting on tail classes compared to large-scale pre-trained models. Our method effectively addresses this issue by utilizing neighbor categories. Besides, even with pre-trained models as initialization, our approach consistently demonstrates satisfactory improvements. For ex-

ample, when using DINOv2 as the backbone, we achieve performance improvements of 5.0%, 2.5%, and 3.1% on the tail classes of ImageNet-LT, iNaturalist, and PlaceLT datasets, respectively, without compromising performance on the head classes. This verifies our method’s generalizability and effectiveness on long-tail datasets.

Fair comparison. We also add auxiliary data to the baseline method. As shown in Tab. 2, RD denotes the random auxiliary data and SD is the data from our selected neighbor categories. The results show that, the randomly auxiliary data significantly degrade the performance during the finetuning stage, and the selected neighbor categories can enhance performance. Moreover, when using our proposed methods with the neighbor categories, the performance can be further boosted. These results validate the effectiveness of both the auxiliary data and our approach.

Can Learning by Category Extrapolation Enhance the State-of-the-Art Methods? We conduct comprehensive experiments with existing SoTAs in Tab. 3, Tab. 4, and Tab. 5. Current methods can be generally categorized into two settings, *i.e.*, training from scratch or adopting CLIP pre-training. We also present results obtained by DINOv2, in which we provide the results of Bal-CE [7] initialized by pre-trained weights from DINOv2. In each pre-training paradigm, we select a SOTA method, and add the same amount of auxiliary data on it, which is denoted by \dagger . Then we implement our proposed method based on the corresponding SoTA methods. The results show that 1) After adding the auxiliary data from neighbor categories, the performance increase. 2) When using the neighbor categories with our proposed methods, we can further enhance the performance. The potential reason is that our method focuses more effectively on learning the features of target classes,

Method	Backbone	Overall	Many	Med.	Few
Training from scratch					
LiVT [40]	ViT-B	76.1	78.9	76.5	74.8
LiVT [†] [40]	ViT-B	77.0	78.8	77.4	75.9
<i>Ours</i>	ViT-B	78.0	78.9	78.2	77.5
Fine-tuning pre-trained model (CLIP)					
LIFT [32]	ViT-B	79.1	72.4	79.0	81.1
LIFT [†] [32]	ViT-B	79.5	72.9	79.4	81.3
<i>Ours</i>	ViT-B	80.9	79.6	80.1	82.1
Fine-tuning pre-trained model (DINOv2)					
Bal-CE [7]	ViT-B	85.0	85.7	86.2	84.2
Bal-CE [†] [7]	ViT-B	85.9	85.8	86.5	85.0
<i>Ours</i>	ViT-B	87.0	86.4	87.4	86.7

Table 4. Performance on iNaturalist 2018. We report accuracy (%) of all methods under three pre-training paradigms.

Method	Backbone	Overall	Many	Med.	Few
Training from scratch					
LiVT [40]	ViT-B	40.8	48.1	40.6	27.5
LiVT [†] [40]	ViT-B	42.8	48.0	42.0	35.1
<i>Ours</i>	ViT-B	43.8	43.7	44.8	41.6
Fine-tuning pre-trained model (CLIP)					
LIFT [32]	ViT-B	51.5	51.3	52.2	50.5
LIFT [†] [32]	ViT-B	51.8	51.5	52.4	51.1
<i>Ours</i>	ViT-B	52.4	51.6	53.0	52.3
Fine-tuning pre-trained model (DINOv2)					
Bal-CE [7]	ViT-B	49.5	49.2	51.3	46.1
Bal-CE [†] [7]	ViT-B	49.9	49.3	51.6	47.3
<i>Ours</i>	ViT-B	50.8	49.4	52.4	49.2

Table 5. Performance on Places-LT. We report accuracy (%) of all methods under three pre-training paradigms.

which avoids being overwhelmed by auxiliary categories. Due to the space limitation, we show more results of previous methods trained with the auxiliary data in Appendix.

4.4. Ablation and Analysis

Contributions of Individual Components. As shown in Tab. 6, we evaluate the contribution of each component of the full method. The baseline is BalCE with DINOv2 pre-training. We conduct ablation experiments on ImageNet-LT. We replace the re-balancing loss (Eq. (2)) with the neighbor-silencing loss (Eq. (4)), obtaining improvements of 1.0% and 1.9% in the medium and tail categories, respectively. If we use the direct classifier instead of retraining the classifier by linear probing, the performance in the medium and tail categories increases to 79.2% and 73.2%, respectively. The best performance is achieved when we do not re-train the classifier and instead directly utilize the classi-

Methods	Many	Medium	Few	Overall
Baseline	84.3	78.3	71.1	79.6
+ Random Category	83.3	75.7	65.4	77.2
+ Neighbor Category	83.8	79.8	73.4	80.5
+ Neighbor Silencing	84.3	80.8	75.3	81.4
+ Direct Classifier	84.7	81.5	76.2	82.0

Table 6. Contributions of individual components. Results are obtained on ImageNet-LT.

fier weights corresponding to the target categories.

The curation of the auxiliary dataset primarily involves three hyper-parameters: the number of auxiliary categories associated with a target category, the maximum number of samples per auxiliary class, and the proportion of the number of auxiliary categories for head (aux_{head}), medium ($\text{aux}_{\text{medium}}$), and tail classes (aux_{tail}), i.e. $\text{aux}_{\text{head}} : \text{aux}_{\text{medium}} : \text{aux}_{\text{tail}}$ (denoted as auxiliary sampling ratio for simplicity). We will analyze these three hyper-parameters separately and fix the other two hyper-parameters individually. The default values for these three hyper-parameters are 5, 50, and 1:1:3, respectively.

Number of Sampled Categories. Fig. 5a studies the effect of the number of auxiliary categories for each target class. The optional values are set to $\{1, 3, 5, 7, 8\}$. We can observe that as the number of neighbor categories increases, the performance gradually improves and finally saturates when approaching 5.

Maximum Number of Sampled Instances Per Class. As shown in Fig. 5b, we study the effect of the number of samples per neighbor category. The optional values are $\{10, 30, 50, 100, 150\}$. If the number of samples collected for a class exceeds the limit, we randomly subsample it to the corresponding number; and if less, we keep them unchanged. It can be seen that as the limit increases to 50, the performance improves. However, when too many instances are included, the performance drops. This can be attributed to an excessive number of samples from auxiliary classes, resulting in an overwhelming of these categories.

Auxiliary Sampling Ratio. Fig. 5c studies the proportion of the number of auxiliary categories for head, medium, and tail classes. When the ratio is 0:1:3, which indicates that the neighbor categories for many classes are removed, we can observe a performance degradation in many classes from 84.4% to 82.3%. This could be because, with only the addition of auxiliary data in the medium and few-shot categories, feature learning tends to skew towards these medium and few-shot categories. Moreover, when we decrease the ratio on medium (ratio=1:0.5:3) and tail (ratio=1:1:1) classes, the performance degrades, respectively.

Visualization. Fig. 6 shows the top-3 PCA components of images sampled from ‘‘Tail’’ classes of ImageNet-LT, where each component is mapped to an RGB channel, and the background is removed by thresholding the first PCA com-

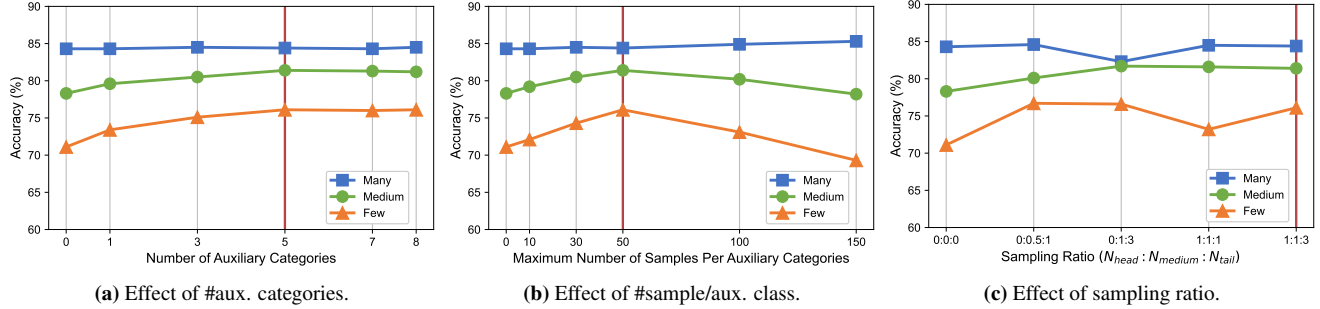


Figure 5. Ablation study on factors related to the curation of auxiliary dataset. Experiments are conducted on ImageNet-LT [20]. Default options are marked in red.

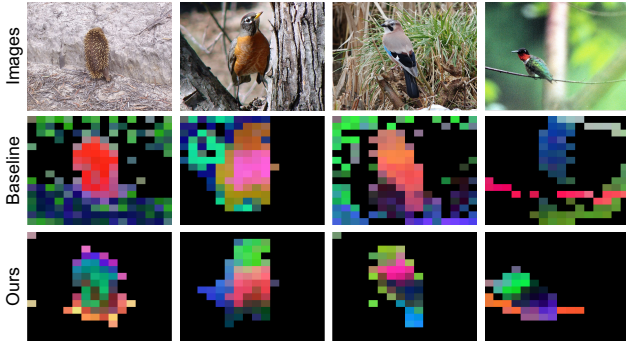


Figure 6. PCA visualization of “Tail” images in ImageNet-LT. Top-3 PCA components of features are mapped to RGB channels, and background is removed by thresholding the first component.

ponent. Both the baseline [7] and our method adopt DINOv2 pre-training. While the baseline finds it hard to locate the object of interest, our method clearly captures better objectness despite the scarcity of “Tail” images.

5. Related Works

Re-Balancing Long-Tail Learning. Class-level re-balancing methods include oversampling training samples from tail classes [3], under-sampling data points from head classes [19], and re-weighting the loss values or gradients based on label frequencies [2, 7] or model’s predictions [17]. Classifier re-balancing mechanisms are based on the finding that uniform sampling on the whole dataset during training benefits representation learning but leads to a biased classifier, so they design specific algorithms to adjust the classifier during or after the representation learning phase [14, 46].

Data Augmentation for Long-Tail Learning. Spatial augmentation methods have performed satisfactorily for representation learning. Among these approaches, Cutout [8] removes random regions, CutMix [42] fills the removed regions with patches from other images, and Mixup series [34, 37, 43] performs convex combination between images. Since data augmentation is closely related to

oversampling, it is also adopted by recent long-tail recognition literature [44, 46]. These techniques, however, are adopted directly while overlooking special data distributions in long-tail learning. Recently, Remix [4] was proposed in favor of the minority classes when mixing samples. Yet, this is still bounded by existing classes. Unlike above, our method samples images from open-set distributions and could greatly benefit from higher data diversity.

Auxiliary Resources for Long-Tail Learning. Previous efforts mainly lie in refining representations with fixed external image features encoded by pre-trained models [13, 21]. The external data could be either the training dataset [21] or crawled from the web [13], and the fusing process could be either non-parametric [21] or learned in an attentive fashion [13]. Besides images, another line [35] is to leverage external textual descriptors encoded by vision-language models [28]. Our method, instead, poses a clear contrast by explicitly introducing external open-set data into a clean training pipeline and is not dependent on any foundation model. There is also a recent work in self-supervised learning that shares the idea of crawling visually-similar data for task-specific improvements [16]. Instead, our work places a special focus on long-tail learning.

6. Concluding Remarks

This paper introduces category extrapolation, which leverages diverse open-set images crawled from the web to enhance closed-set long-tail learning. In addition to a clean and decent method that shows superior performance on “Medium” and “Few” splits across standard benchmarks, we also provide instrumental guidance on when the auxiliary data helps most and empirical explanations on how they help shape the feature manifold through visualizations. We hope our research will attract more researchers to consider how to leverage additional data to address the pervasive problem in long-tail learning. Related research topics could include (i) what kind of additional data is more compatible with target datasets and (ii) how to take the additional data in conjunction with target datasets for training.

References

- [1] Shaden Alshammari, Yu-Xiong Wang, Deva Ramanan, and Shu Kong. Long-tailed recognition via weight balancing. In *CVPR*, 2022. 1
- [2] Kaidi Cao, Colin Wei, Adrien Gaidon, Nikos Arechiga, and Tengyu Ma. Learning imbalanced datasets with label-distribution-aware margin loss. In *NeurIPS*, 2019. 8
- [3] Nitesh V Chawla, Kevin W Bowyer, Lawrence O Hall, and W Philip Kegelmeyer. Smote: synthetic minority over-sampling technique. *JAIR*, 2002. 1, 8
- [4] Hsin-Ping Chou, Shih-Chieh Chang, Jia-Yu Pan, Wei Wei, and Da-Cheng Juan. Remix: rebalanced mixup. In *ECCV Workshops*, 2020. 1, 8
- [5] Ekin D Cubuk, Barret Zoph, Jonathon Shlens, and Quoc V Le. Randaugment: Practical automated data augmentation with a reduced search space. In *CVPR Workshops*, 2020. 5
- [6] Jiequan Cui, Zhisheng Zhong, Shu Liu, Bei Yu, and Jiaya Jia. Parametric contrastive learning. In *ICCV*, 2021. 1
- [7] Yin Cui, Menglin Jia, Tsung-Yi Lin, Yang Song, and Serge Belongie. Class-balanced loss based on effective number of samples. In *CVPR*, 2019. 1, 2, 3, 5, 6, 7, 8
- [8] Terrance DeVries and Graham W Taylor. Improved regularization of convolutional neural networks with cutout. *arXiv:1708.04552*, 2017. 1, 8
- [9] Bowen Dong, Pan Zhou, Shuicheng Yan, and Wangmeng Zuo. LPT: Long-tailed prompt tuning for image classification. In *ICLR*, 2023. 1
- [10] Alexey Dosovitskiy, Lucas Beyer, Alexander Kolesnikov, Dirk Weissenborn, Xiaohua Zhai, Thomas Unterthiner, Mostafa Dehghani, Matthias Minderer, Georg Heigold, Sylvain Gelly, Jakob Uszkoreit, and Neil Houlsby. An image is worth 16x16 words: Transformers for image recognition at scale. In *ICLR*, 2021. 1, 3, 5
- [11] Kaiming He, Xiangyu Zhang, Shaoqing Ren, and Jian Sun. Deep residual learning for image recognition. In *CVPR*, 2016. 1
- [12] Yin-Yin He, Jianxin Wu, and Xiu-Shen Wei. Distilling virtual examples for long-tailed recognition. In *ICCV*, 2021. 1
- [13] Ahmet Iscen, Alireza Fathi, and Cordelia Schmid. Improving image recognition by retrieving from web-scale image-text data. In *CVPR*, 2023. 8
- [14] Bingyi Kang, Saining Xie, Marcus Rohrbach, Zhicheng Yan, Albert Gordo, Jiashi Feng, and Yannis Kalantidis. Decoupling representation and classifier for long-tailed recognition. In *ICLR*, 2020. 2, 5, 8
- [15] Ivan Krasin, Tom Duerig, Neil Alldrin, Vittorio Ferrari, Sami Abu-El-Hajja, Alina Kuznetsova, Hassan Rom, Jasper Uijlings, Stefan Popov, Andreas Veit, Serge Belongie, Victor Gomes, Abhinav Gupta, Chen Sun, Gal Chechik, David Cai, Zheyun Feng, Dhyanesh Narayanan, and Kevin Murphy. Openimages: A public dataset for large-scale multi-label and multi-class image classification. *Dataset available from <https://github.com/openimages>*, 2017. 3
- [16] Alexander C Li, Ellis Brown, Alexei A Efros, and Deepak Pathak. Internet explorer: Targeted representation learning on the open web. In *ICML*, 2023. 8
- [17] Tsung-Yi Lin, Priya Goyal, Ross Girshick, Kaiming He, and Piotr Dollár. Focal loss for dense object detection. In *ICCV*, 2017. 8
- [18] Jiahui Liu, Xin Wen, Shizhen Zhao, Yingxian Chen, and Xiaojuan Qi. Can ood object detectors learn from foundation models? In *ECCV*, 2025. 1
- [19] Xu-Ying Liu, Jianxin Wu, and Zhi-Hua Zhou. Exploratory undersampling for class-imbalance learning. In *ICDM*, 2006. 8
- [20] Ziwei Liu, Zhongqi Miao, Xiaohang Zhan, Jiayun Wang, Boqing Gong, and Stella X Yu. Large-scale long-tailed recognition in an open world. In *CVPR*, 2019. 2, 3, 5, 8
- [21] Alexander Long, Wei Yin, Thalaiyasingam Ajanthan, Vu Nguyen, Pulak Purkait, Ravi Garg, Alan Blair, Chunhua Shen, and Anton van den Hengel. Retrieval augmented classification for long-tail visual recognition. In *CVPR*, 2022. 8
- [22] Ilya Loshchilov and Frank Hutter. Decoupled weight decay regularization. In *ICLR*, 2019. 5
- [23] Oquab Maxime, Darcet Timothée, Moutakanni Théo, Vo Huy, Szafraniec Marc, Khalidov Vasil, Fernandez Pierre, Haziza Daniel, Massa Francisco, El-Nouby Alaaeldin, Assran Mahmoud, Ballas Nicolas, Galuba Wojciech, Howes Russell, Huang Po-Yao, Li Shang-Wen, Misra Ishan, Rabbat Michael, Sharma Vasu, Synnaeve Gabriel, Xu Hu, Jegou Hervé, Mairal Julien, Labatut Patrick, Joulin Armand, and Bojanowski Piotr. DINOv2: Learning robust visual features without supervision. *arXiv:2304.07193*, 2023. 2, 3, 4, 5
- [24] Leland McInnes, John Healy, and James Melville. UMAP: Uniform manifold approximation and projection for dimension reduction. *arXiv:1802.03426*, 2020. 3
- [25] OpenAI. GPT-4 technical report. *arXiv:2303.08774*, 2023. 4
- [26] Sarah Parisot, Pedro M Esperança, Steven McDonagh, Tamas J Madarasz, Yongxin Yang, and Zhenguo Li. Long-tail recognition via compositional knowledge transfer. In *CVPR*, 2022. 1
- [27] Seulki Park, Youngkyu Hong, Byeongho Heo, Sangdoon Yun, and Jin Young Choi. The majority can help the minority: Context-rich minority oversampling for long-tailed classification. In *CVPR*, 2022. 1
- [28] Alec Radford, Jong Wook Kim, Chris Hallacy, Aditya Ramesh, Gabriel Goh, Sandhini Agarwal, Girish Sastry, Amanda Askell, Pamela Mishkin, Jack Clark, et al. Learning transferable visual models from natural language supervision. In *ICML*, 2021. 2, 5, 8
- [29] Tal Ridnik, Emanuel Ben-Baruch, Asaf Noy, and Lihi Zelnik-Manor. Imagenet-21k pretraining for the masses, 2021. 3
- [30] Olga Russakovsky, Jia Deng, Hao Su, Jonathan Krause, Sanjeev Satheesh, Sean Ma, Zhiheng Huang, Andrej Karpathy, Aditya Khosla, Michael Bernstein, Alexander C. Berg, and Li Fei-Fei. ImageNet Large Scale Visual Recognition Challenge. *IJCV*, 2015. 5
- [31] Dvir Samuel and Gal Chechik. Distributional robustness loss for long-tail learning. In *ICCV*, 2021. 1
- [32] Jiang-Xin Shi, Tong Wei, Zhi Zhou, Jie-Jing Shao, Xin-Yan Han, and Yu-Feng Li. Long-tail learning with foundation model: Heavy fine-tuning hurts. In *ICML*, 2024. 6, 7

- [33] Karen Simonyan and Andrew Zisserman. Very deep convolutional networks for large-scale image recognition. In *ICLR*, 2015. 1
- [34] Cecilia Summers and Michael J Dinneen. Improved mixed-example data augmentation. In *WACV*, 2019. 8
- [35] Changyao Tian, Wenhai Wang, Xizhou Zhu, Jifeng Dai, and Yu Qiao. VL-LTR: learning class-wise visual-linguistic representation for long-tailed visual recognition. In *ECCV*, 2022. 8
- [36] Grant Van Horn, Oisin Mac Aodha, Yang Song, Yin Cui, Chen Sun, Alex Shepard, Hartwig Adam, Pietro Perona, and Serge Belongie. The inaturalist species classification and detection dataset. In *CVPR*, 2018. 2, 3, 5
- [37] Vikas Verma, Alex Lamb, Christopher Beckham, Amir Najafi, Ioannis Mitliagkas, David Lopez-Paz, and Yoshua Bengio. Manifold mixup: Better representations by interpolating hidden states. In *ICML*, 2019. 8
- [38] Xudong Wang, Long Lian, Zhongqi Miao, Ziwei Liu, and Stella X Yu. Long-tailed recognition by routing diverse distribution-aware experts. In *ICLR*, 2021. 1
- [39] Liuyu Xiang, Guiguang Ding, Jungong Han, et al. Learning from multiple experts: Self-paced knowledge distillation for long-tailed classification. In *ECCV*, 2020. 1
- [40] Zhengzhuo Xu, Ruikang Liu, Shuo Yang, Zenghao Chai, and Chun Yuan. Learning imbalanced data with vision transformers. In *CVPR*, 2023. 5, 6, 7
- [41] Sihao Yu, Jiafeng Guo, Ruqing Zhang, Yixing Fan, Zizhen Wang, and Xueqi Cheng. A re-balancing strategy for class-imbalanced classification based on instance difficulty. In *CVPR*, 2022. 1
- [42] Sangdoon Yun, Dongyoon Han, Seong Joon Oh, Sanghyuk Chun, Junsuk Choe, and Youngjoon Yoo. Cutmix: Regularization strategy to train strong classifiers with localizable features. In *ICCV*, 2019. 1, 5, 8
- [43] Hongyi Zhang, Moustapha Cisse, Yann N. Dauphin, and David Lopez-Paz. mixup: Beyond empirical risk minimization. In *ICLR*, 2018. 1, 5, 8
- [44] Zhisheng Zhong, Jiequan Cui, Shu Liu, and Jiaya Jia. Improving calibration for long-tailed recognition. In *CVPR*, 2021. 1, 8
- [45] Bolei Zhou, Agata Lapedriza, Aditya Khosla, Aude Oliva, and Antonio Torralba. Places: A 10 million image database for scene recognition. *IEEE TPAMI*, 2017. 5
- [46] Boyan Zhou, Quan Cui, Xiu-Shen Wei, and Zhao-Min Chen. BBN: Bilateral-branch network with cumulative learning for long-tailed visual recognition. In *CVPR*, 2020. 2, 5, 8
- [47] Jiangang Zhu, Zheng Wang, Jingjing Chen, Yi-Ping Phoebe Chen, and Yu-Gang Jiang. Balanced contrastive learning for long-tailed visual recognition. In *CVPR*, 2022. 1